Spatial depolarization of light from the bulks: electromagnetic prediction

Myriam Zerrad, Hervé Tortel, Gabriel Soriano, Ayman Ghabbach and Claude Amra

Aix Marseille Université, CNRS, Centrale Marseille, Institut Fresnel, UMR 7249, 13013 Marseille, France
**myriam.zerrad@fresnel.fr*

Abstract: The spatial depolarization of light emitted by heterogeneous bulks is predicted with exact electromagnetic theories. The sample microstructure and geometry is connected with partial polarization.

OCIS codes: (030.6140) Speckle; (260.2130) Ellipsometry and polarimetry; (260.5430) Polarization; (290.5855) Scattering, polarization; (120.2130) Ellipsometry and polarimetry.

References and links

1. O. V. Angelsky, S. G. Hanson, C. Y. Zenkova, M. P. Gorsky, and N. V. Gorodyns'ka, "On polarization metrology (estimation) of the degree of coherence of optical waves," Opt. Express **17**(18), 15623–15634 (2009).
2. C. Brosseau, *Fundamentals of Polarized Light - A Statistical Approach* (Wiley, 1998).
3. E. Wolf, *Theory of coherence and polarization of light* (Cambridge University Press, 2007).
4. E. Wolf and L. Mandel, *Optical Coherence and Quantum Optics* (Cambridge University Press, 1995).
5. R. Martnez-Herrero, P. M. Mejas, and G. Piquero, *Characterization of Partially Polarized Light Fields* (Springer, 2009).
6. E. Jakeman and K. D. Ridley, *Modeling Fluctuations in Scattered Waves* (Taylor and Francis Group, 2006).
7. I. Mokhun, "Introduction to linear singular optics," in *Optical Correlation Techniques and Applications*, O. V. Angelsky, ed. (SPIE press, USA, 2007).
8. E. Wolf, "Unified theory of Coherence and polarization of random electromagnetic beams," Phys. Lett. A **312**(5-6), 263–267 (2003).
9. P. Réfrégier and F. Goudail, "Invariant degrees of coherence of partially polarized light," Opt. Express **13**(16), 6051–6060 (2005).
10. C. Amra, M. Zerrad, L. Siozade, G. Georges, and C. Deumié, "Partial polarization of light induced by random defects at surfaces or bulks," Opt. Express **16**(14), 10372–10383 (2008).
11. M. Zerrad, J. Sorrentini, G. Soriano, and C. Amra, "Gradual loss of polarization in light scattered from rough surfaces: Electromagnetic prediction," Opt. Express **18**(15), 15832–15843 (2010).
12. J. Broky and A. Dogariu, "Correlations of polarization in random electro-magnetic fields," Opt. Express **19**(17), 15711–15719 (2011).
13. G. Soriano, M. Zerrad, and C. Amra, "Enpolarization and depolarization of light scattered from chromatic complex media," Opt. Express **22**(10), 12603–12613 (2014).
14. J. Sorrentini, M. Zerrad, G. Soriano, and C. Amra, "Enpolarization of light by scattering media," Opt. Express **19**(22), 21313–21320 (2011).
15. M. Zerrad, G. Soriano, A. Ghabbach, and C. Amra, "Light enpolarization by disordered media under partial polarized illumination: The role of cross-scattering coefficients," Opt. Express **21**(3), 2787–2794 (2013).
16. J. Li, G. Yao, and L. V. Wang, "Degree of polarization in laser speckles from turbid media: implications in tissue optics," J. Biomed. Opt. **7**(3), 307–312 (2002).
17. A. Ghabbach, M. Zerrad, G. Soriano, and C. Amra, "Accurate metrology of polarization curves measured at the speckle size of visible light scattering," Opt. Express **22**(12), 14594–14609 (2014).
18. A. Ghabbach, M. Zerrad, G. Soriano, S. Liukaityte, and C. Amra, "Depolarization and enpolarization DOP histograms measured for surface and bulk speckle patterns," Opt. Express **22**(18), 21427–21440 (2014).
19. J. Sorrentini, M. Zerrad, and C. Amra, "Statistical signatures of random media and their correlation to polarization properties," Opt. Lett. **34**(16), 2429–2431 (2009).
20. J. M. Elson and J. M. Bennett, "Relation between the angular dependence of scattering and the statistical properties of optical surfaces," J. Opt. Soc. Am. **69**(1), 31–47 (1979).
21. C. Amra, "Light scattering from multilayer optics. I. Tools of investigation," J. Opt. Soc. Am. A **11**(1), 197–210 (1994).
22. C. Amra, "Light scattering from multilayer optics. II. Application to experiment," J. Opt. Soc. Am. A **11**(1), 211–226 (1994).
23. C. Amra, "First-order vector theory of bulk scattering in optical multilayers," J. Opt. Soc. Am. A **10**(2), 365–374 (1993).

#228254 - $15.00 USD Received 12 Dec 2014; revised 27 Feb 2015; accepted 4 Mar 2015; published 23 Mar 2015

24. M. Zerrad, M. Lequime, S. Liukaityte, and C. Amra, "Spatially-resolved surface topography retrieved from far-field intensity scattering measurements," in *Optical Interference Coatings*, M. a. R. D. Tilsch, ed. (Optical Society of America, 2013), p. ThC.9.
25. R. Brandel, A. Mokhun, I. Mokhun, and J. Viktorovskaya, "Fine structure of heterogeneous vector field and his space averaged polarization characteristics.," (Opt. Appl., 2006), pp. 79–95.
26. M. Zerrad, J. Sorrentini, G. Soriano, and C. Amra, "Multiscale spatial depolarization of light: electromagnetism and statistical optics," in *Physical Optics*, D. G. Smith, F. Wyrowski, and Andreas Erdmann, eds. (Proceedings of SPIE, 2011).
27. J. W. Goodman, *Speckle Phenomena in Optics: Theory and Applications* (Roberts and Company Publishers, 2007).
28. L. Mandel and E. Wolf, eds., *Optical Coherence and Quantum Optics* (Cambridge University Press 1995).
29. G. Soriano, M. Zerrad, and C. Amra, "Mapping the coherence time of far-field speckle scattered by disordered media," Opt. Express **21**(20), 24191–24200 (2013).
30. L. Tsang, J. A. Kong, and K.-H. Ding, *Scattering of Electromagnetic Waves: Numerical Simulations* (Wiley-Interscience, 2001).
31. I. Freund, M. Rosenbluh, and S. Feng, "Memory effects in propagation of optical waves through disordered media," Phys. Rev. Lett. **61**(20), 2328–2331 (1988).
32. O. Katz, E. Small, and Y. Silberberg, "Looking around corners and through thin turbid layers in real time with scattered incoherent light," Nat. Photonics **6**(8), 549–553 (2012).
33. A. P. Mosk, A. Lagendijk, G. Lerosey, and M. Fink, "Controlling waves in space and time for imaging and focusing in complex media," Nat. Photonics **6**(5), 283–292 (2012).
34. O. Cmielewski, H. Tortel, A. Litman, and M. Saillard, "A two step procedure for obstacle characterization under a rough surface," IEEE Trans. Geosci. Rem. Sens. **45**, 2850–2858 (2007).
35. A. F. Peterson, L. R. Scott, and R. Mittra, *Computational Method for Electromagnetics* (Wiley-IEEE Press Oxford Univeristy Press, 1998).
36. J. Jin, *The Finite Element Method in Electromagnetics* (John Wiley & Sons, Inc, 2002).
37. P. Godard, "Optique électromagnétique non-linéaire polyharmonique: théorie et modélisation numérique," in *PhD thesis* (Université de Provence, Marseille, France, 2009).
38. C. Geuzaine and J. F. Remacle, "GMSH A three dimensional finite element mesh generator with built-in pre- and post-processing facilities," Int. J. Numer. Methods Eng. **79**, 1309–1331 (2009).

Introduction

Light polarization and coherence [1–7] have become the focus of numerous works, and were accompanied by the emergence of unified theories [8, 9]. Additional complexity was brought by the introduction of random media, hence mixing spatial and temporal disorders [10–12]. Specific effects were recently emphasized at the speckle size, like the local (temporal) en-polarization of light [13–15], and the multi-scale (spatial) depolarization [11, 12, 16]. Most effects were confirmed by experiment [16–19], which justifies a motivation to go further in these fields.

Far field light scattering has been a powerful tool for decades to analyze complex or random media. For small disturbed media, perturbative theories have shown how the emitted pattern was driven by the Fourier transform of the surface roughness [20–22] or the bulk heterogeneity [23], a result which allowed to directly solve inverse problems and characterize substrates and optical coatings [22, 24]. Arbitrary scattering regimes are much more complex to analyze, due to the presence of integral or coupled equations which connect the fields at different spatial frequencies. In all situations the behavior of the far field pattern is intimately connected with the sample microstructure, which drives the angular, spectral and polarization properties. Recent examples give a detailed analysis of the polarization degree at the speckle size in the far field [11, 12, 16, 25], and emphasize spatial depolarization [11, 16, 26] and temporal repolarization [14, 15] of light, all phenomena which strongly depend on the samples microstructure (roughness, inhomogeneity). Applications were also found for biological tissues and others.

Indeed prediction of the polarization process in disordered media often involve a phenomenological approach, similar to that of Goodman's phasor model [27] with partially or fully developed speckles. Such description of the scattering process is very practical and allowed to reveal unexpected phenomena such as the en-polarization process [14, 15]; also, it allowed to predict a spectral depolarization [3, 28] responsible for strong modification of the polarization degree (dop) histograms [13], as well as the modification of time coherence [29]

#228254 - $15.00 USD Received 12 Dec 2014; revised 27 Feb 2015; accepted 4 Mar 2015; published 23 Mar 2015

in disordered media. However this phenomenological model is valid for highly heterogeneous samples and fails at intermediate electromagnetic regimes, whereas these regimes occur in numerous situations. As an example, electromagnetic theories predict the scattering coefficients to be strongly inter-dependent, except for extreme situations where they can be considered uncorrelated; these last situations are those of highly heterogeneous samples currently described with the phasor model.

Within this framework there is a current need to introduce exact values of the scattering coefficients in the calculation of the polarization process, that is, to provide a more exact link between the sample microstructure and the scattering coefficients. Such data would allow to analyze the gradual transition of polarization degree from a slightly heterogeneous sample to a highly heterogeneous one, hence providing a signature of the complex media together with a key information for optical imaging through these media.

We already performed [11] this kind of study for rough surfaces, that is, for surface scattering. For that we used an exact electromagnetic model based on the frontier integral [30]. Numerical results allowed to emphasize the multi-scale nature of the spatial polarization degree of the speckle emitted by surfaces of increasing slopes or root-mean-squares [11]. In other words, depending on the surface characteristics, it is possible to know from which receiver aperture full polarization starts to fail, due a spatial average process. The theoretical model was one-dimensional since time consuming is prohibitive for high slope 2D surfaces.

However to our knowledge the similar bulk problem has not yet been addressed, even though the analysis of bulk media constitutes a relevant topic for imaging in diffuse environment [31–33]. One question concerns the number of speckle grains whose integration cancels polarization, and the result will depend on the statistics and amplitude of the heterogeneity. To solve this point, an exact electromagnetic bulk model is required to calculate the volume scattering coefficients with accuracy, and to introduce them within the calculation of polarization degree (dop). Compared to the surface problem, this requirement is much more difficult to satisfy, because the basic bulk problem is necessarily at least bi-dimensional, and because the bulk/light interaction involves a larger region (not limited to the surfaces).

Hence this paper is an extension to the bulks of previous works [11] devoted to surface scattering. Here we use an exact electromagnetic model of bulk scattering (based on finite elements) to emphasize the gradual relationship between the sample bulk microstructure and the spatial polarization degree at the speckle size. Diagrams are plotted to emphasize the dispersion of polarization states on the Poincaré sphere, and to calculate the spatial dop versus the bulk heterogeneity. Results allow to calibrate the spatial depolarization process versus sample microstructure (thickness, index heterogeneity), with applications in most polarimetric techniques involved in imaging and diffusive media, spatial and defense, biomedical and biophotonics...

Principles of spatial depolarization

We start with a brief recall on spatial (global) depolarization, not to be confused with temporal (local) depolarization [3, 11, 19]. Indeed the incident light is assumed to be collimated, fully polarized and coherent (perfectly monochromatic), a situation where temporal depolarization does not occur. The analytical signal of the electromagnetic field is described by two complex polarization modes E_S^0 and E_P^0. With two non-zero modes (non-linear polarization), the full polarization (temporal and local) of the incident field is equivalent to a unity modulus of the complex correlation coefficient μ_0 given by:

$$\mu_0(\boldsymbol{\rho}) = \frac{1}{\alpha_0}\left\langle E_S^0(\boldsymbol{\rho},t)\,E_P^{0*}(\boldsymbol{\rho},t)\right\rangle_t \qquad (1)$$

#228254 - $15.00 USD Received 12 Dec 2014; revised 27 Feb 2015; accepted 4 Mar 2015; published 23 Mar 2015

with $\langle\rangle_t$ the temporal average, * the complex conjugate, $\boldsymbol{\rho}$ the space coordinates and α the normalization coefficient:

$$\alpha_0(\boldsymbol{\rho})^2 = \left\langle \left|E_S^0(\boldsymbol{\rho},t)\right|^2 \right\rangle_t \left\langle \left|E_P^0(\boldsymbol{\rho},t)\right|^2 \right\rangle_t \tag{2}$$

Therefore the incident light here follows: $|\mu_0| = 1 => \text{dop} = 1$, with dop the polarization degree.

As for the scattered field denoted (E_S, E_P), it can be written as the product of the incident field by the scattering matrix (ν_{ij}):

$$\begin{pmatrix} E_S \\ E_P \end{pmatrix}(\rho,t) = \begin{pmatrix} \nu_{SS}(\rho) & \nu_{PS}(\rho) \\ \nu_{SP}(\rho) & \nu_{PP}(\rho) \end{pmatrix} \begin{pmatrix} E_S^0 \\ E_P^0 \end{pmatrix}(\rho,t) \tag{3}$$

with ν_{ij} the scattering coefficients [19]. This last relationship is valid under the assumption of achromatic scattering coefficients within the laser band-pass [13], in accordance with the assumption of a perfectly monochromatic source.

In a second step the complex correlation coefficient of the scattered field can be classically written as:

$$\mu(\boldsymbol{\rho}) = \frac{1}{\alpha}\left\langle E_S(\boldsymbol{\rho},t)\, E_P^*(\boldsymbol{\rho},t)\right\rangle_t \tag{4}$$

with:

$$\alpha^2 = \left\langle \left|E_S(\boldsymbol{\rho},t)\right|^2 \right\rangle_t \left\langle \left|E_P(\boldsymbol{\rho},t)\right|^2 \right\rangle_t \tag{5}$$

Previous works [11, 13, 15] have shown that because the illumination is perfectly monochromatic and fully polarized, full temporal polarization is guaranteed for the scattered field at any space location, so that temporal averages vanish in Eq. (4) and mutual coherence of the scattered field can be turned as:

$$\mu(\boldsymbol{\rho}) = \frac{E_S(\boldsymbol{\rho})\, E_P^*(\boldsymbol{\rho})}{\sqrt{\left|E_S(\boldsymbol{\rho})\right|^2 \left|E_P(\boldsymbol{\rho})\right|^2}} \quad \Rightarrow \quad |\mu| = 1 \tag{6}$$

In other words, as illustrated Fig. 1, a fully polarized monochromatic illumination creates a fully polarized speckle pattern. As a consequence, any depolarization effect will be the result of spatial (not temporal) depolarization, that is, the result of an average process of all full polarization states collected within the receiver aperture. In Fig. 1 for instance, the resulting polarization degree will approach zero, due to the random variation of polarization states from one speckle grain to another. However in the general case the correlation length of polarization measured over the speckle grains will depend on the bulk microstructure, what we calculate in the next sections.

#228254 - $15.00 USD Received 12 Dec 2014; revised 27 Feb 2015; accepted 4 Mar 2015; published 23 Mar 2015

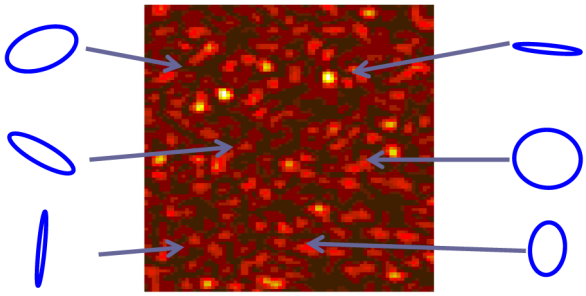

Fig. 1. Dispersion of polarization state within a spatially depolarizing speckle pattern- Schematic view.

Such spatial depolarization is quantitatively defined in a way similar to temporal depolarization, which means that temporal averages are completed by spatial averages. However while temporal average involves a unique scale due to full time integration by the low band-pass optical detectors in the visible range, the spatial average depends on the detection area and hence requires a multi-scale analysis. As a consequence, the complex correlation is extended to a function of the detector aperture $\Delta\Omega$ as follows [11, 16]:

$$\mu(\boldsymbol{\rho},\Delta\Omega)=\frac{\left\langle E_S(\boldsymbol{\rho})E_P^*(\boldsymbol{\rho})\right\rangle_{\Delta\Omega}}{\alpha(\Delta\Omega)} \tag{7}$$

with:

$$\alpha^2(\Delta\Omega)=\left\langle\left|E_S(\boldsymbol{\rho},\Delta\Omega)\right|^2\right\rangle_{\Delta\Omega}\left\langle\left|E_P(\boldsymbol{\rho},\Delta\Omega)\right|^2\right\rangle_{\Delta\Omega} \tag{8}$$

So, the usual matrix formalism can be used from now, and we consider the multi-scale degree of polarization *(MDOP)* defined Eq. (9) as the measurable quantity below:

$$MDOP(\rho,\Delta\Omega)=\sqrt{1-4\frac{\det\left\{J(\rho,\Delta\Omega)\right\}}{\left[tr\left\{J(\rho,\Delta\Omega)\right\}\right]^2}} \tag{9}$$

where J is the coherence matrix:

$$J(\rho,\Delta\Omega)=\begin{pmatrix}\left\langle(E_S)^*E_S\right\rangle_{\Delta\Omega} & \left\langle(E_S)^*E_P\right\rangle_{\Delta\Omega}\\ \left\langle(E_P)^*E_S\right\rangle_{\Delta\Omega} & \left\langle(E_P)^*E_P\right\rangle_{\Delta\Omega}\end{pmatrix} \tag{10}$$

The next step in this paper will be to calculate the MDOP function emitted by bulk heterogeneities.

The electromagnetic bulk scattering model

In order to avoid a phenomenological model limited to extreme regimes of heterogeneity, we quantify the MDOP with an exact electromagnetic method. To cover most scattering regimes from perturbative inhomogeneities to the resonant domain, a rigorous solution of Maxwell's equations is required. Moreover the complex scattered fields must be perfectly known at all directions in the far field at a speckle size; for this reason the numerical approach has to be quite fast, and we restrict ourselves to the case of two dimensional volumes *n=f(x,z)*, with z the normal direction, which means that the geometry is invariant along the *y* axis.

#228254 - $15.00 USD Received 12 Dec 2014; revised 27 Feb 2015; accepted 4 Mar 2015; published 23 Mar 2015

The problem that we solve at hand is the following. We consider a plane interface at the separation (z = 0) of two non-magnetic materials. The superstrate (incident medium) is air while the substrate is an heterogeneous medium of arbitrary thickness d, with a variation n(x,z) of refractive index for 0 < z < d. For z > d the medium has a constant refractive index of 1, identical to that of the superstrate.

This structure is illuminated by a linearly polarized incident wave (s or p polarization) coming from z = -∞. The incident field is assumed to be an approximate gaussian beam and is represented by a finite sum of plane waves. If u^t designates the tangential component of the total field *i.e.* E^t or H^t for respectively s or p polarization, it follows the equation:

$$div\left(\xi\ grad\left(u^t\right)\right)+\omega_0^2\varepsilon_0\mu_0\chi u^t=0 \tag{11}$$

where, for s polarization:

$$\begin{cases}\xi=\dfrac{1}{\mu(x,z)}=\dfrac{1}{\mu_0}\\ \chi=\varepsilon(x,z)\\ u=E(x,z)\end{cases} \tag{12}$$

and, for p polarization:

$$\begin{cases}\xi=\dfrac{1}{\varepsilon(x,z)}\\ \chi=\mu(x,z)=\mu_0\\ u=H(x,y)\end{cases} \tag{13}$$

For both polarizations the incident field satisfies the following homogeneous Helmholtz equation:

$$div\left(\xi grad\left(u^i\right)\right)+\omega_0^2\varepsilon_0\mu_0\chi u^i=0 \tag{14}$$

With:

$$\chi_0=1\quad\&\quad\xi_0=1 \tag{15}$$

On the other hand the scattered field u^S **,** which we define as:

$$u^t=u^S+u^i \tag{16}$$

satisfies a radiation condition at infinity.

In order to solve this kind of scattering problem we have first pursued the development of an already existing home made FEM (Finite Elements Method) software based on the resolution of the weak form of the Helmholtz equation and used in different configurations [34]. In this software the unknowns are expanded onto P_1 Lagrange basis functions associated to a conformal triangular mesh of the scene. The amplitude of the scattered field in a given direction is then computed thanks to the Huygens principle. One of the key point of this method is to properly introduce the sources responsible for the incident field. In the case of an incident field of finite extent, the use of a Bayliss-Turkell boundary conditions on the external boundary yields a good approximation of the incident field [35]. Another method consists in

#228254 - $15.00 USD Received 12 Dec 2014; revised 27 Feb 2015; accepted 4 Mar 2015; published 23 Mar 2015

using a scattered field formulation [36] of the problem where a reference field calculated in a closed form way is associated to a geometrical configuration of the setup. In that case the total field can be written as:

$$u^t = u^S + u^{ref} \tag{17}$$

and satisfies the following equation:

$$div\left(\xi\ grad\left(u^S\right)\right) + \omega_0^2 \varepsilon_0 \mu_0 \chi u^S = div\left\{\left(\xi_{ref} - \xi\right).grad\left(u^S\right)\right\} + \omega_0^2 \varepsilon_0 \mu_0 \left(\chi_{ref} - \chi\right).u^{ref} \tag{18}$$

In this problem we have used the principle of virtual antennas [37] where we are first looking for an equivalent current distribution which produces the same incident field u^i in the computational domain Ω. From a mathematical point of view we want to find j_Γ which verifies:

$$div\left(\xi\ grad\left(u^t\right)\right) + \omega_0^2 \varepsilon_0 \mu_0 \chi u^i = -j\omega_0 \mu_0 j_\Gamma \delta_\Gamma \quad in \quad \Omega \tag{19}$$

where Γ is the border of the domain at $z = z_\Gamma$.

In the s polarization case, if one substitutes the whole domain Ω by a perfect electric conductor the current distribution produced by the incident Gaussian beam on Γ is such that it produces a null field inside Ω. If one takes j_Γ equal to:

$$j_\Gamma = \frac{1}{i\omega_0 \mu_0} \left[\frac{\partial u^{pec}}{\partial n} \right]_\Gamma \tag{20}$$

where the value between brackets is corresponding to the jump of the normal derivative of u^{pec} at Γ when Ω is substituted by a perfect electric conductor. The field generated by this current distribution is equal to u^i for $z < z_\Gamma$, satisfies a radiation boundary condition and then can be cancelled out by a classical PML for $z > z_\Gamma$.

The same kind of result can be obtained for p polarization by using duality principle and assuming in this case that Ω is a perfect magnetic conductor.

Numerical considerations

The domain Ω is a rectangle with size typically equal to $100\lambda \times 50\ \lambda$. A free unstructured mesh generator [38] (gmsh©) is used to dicretize the whole domain. P_1 Lagrange basis functions are used to discretize the field. The sparse system is solved thanks to a sequential direct sparse solver MUMPS (MUMPS©). The discretization of the whole domain gives around 3.10^6 degrees of freedom in the linear system. This system is solved in more or less 8 min. per configuration and its resolution uses around 10 GB of RAM.

The computation time for the near to far field transformation is negligible regarding the time spent in the resolution of the linear system. Comparisons of the scattered field thanks to this method with respect to analytical expressions in case of an homogeneous substrate have shown an excellent agreement between both methods.

Bulk and scattering characteristics

Phase and amplitude of the electromagnetic field scattered by a panel of arbitrary 2D volumes were calculated for the two polarization modes *S* and *P*, where the electric *(S)* or the magnetic *(P)* field is along the invariant y-direction, with z the average sample normal. The bulks are realizations of a stationary stochastic process with Gaussian heterogeneities distribution; also, they have Gaussian autocorrelation functions in both x and z directions. As such, the bulks are

#228254 - $15.00 USD Received 12 Dec 2014; revised 27 Feb 2015; accepted 4 Mar 2015; published 23 Mar 2015

statistically characterized by the relative index inhomogeneity $\delta_n/|\overline{n}|$ defined Eq. (21), and by their correlation lengths L_x and L_z in both $_x$ and $_z$ directions. Concerning the bulk geometry, it is 100 λ long while its depth varies in the range 0.1λ to 20 λ . It is illuminated with a Gaussian beam under 15° incidence angle at an arbitrary wavelength λ. The inhomogeneities are assumed to be dielectric (real Δn) and engraved in fused silica whose real refractive index is $\overline{n}$ = 1.49 at this wavelength.

$$\frac{\delta_n}{|\overline{n}|} = \sqrt{\left\langle \left| \frac{\Delta n}{\overline{n}} \right|^2 \right\rangle_{x,z}} = \sqrt{\frac{1}{d_x d_z} \iint_{x,z} \left| \frac{\Delta n(x,z)}{\overline{n}} \right|^2 dxdz} \qquad (21)$$

with $d_x = 100\lambda$ and $d_z = d$ the thickness. As an illustration, three examples of cartography with increasing heterogeneities were generated for the optical indices in Fig. 2.

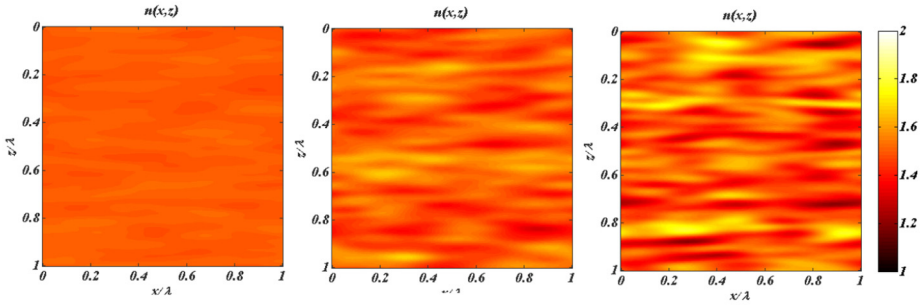

Fig. 2. Example of inhomogeneous bulk (δ_n / n = 10^{-2}, 5.10^{-1} and 10^{-1}).

The complex polarized modes E_S and E_P of the scattered field are then calculated for 1800 scattering angles in the θ angular range *(0°,180°)* and regularly sampled with a step $\delta\theta = 0.1^\circ$.

For each root mean square value of the index heterogeneity, we calculated the corresponding mean value of the Total Integrated Scattering (TIS) versus the layer thickness. Results are given in Fig. 3. The mean free paths L are also given for these samples.

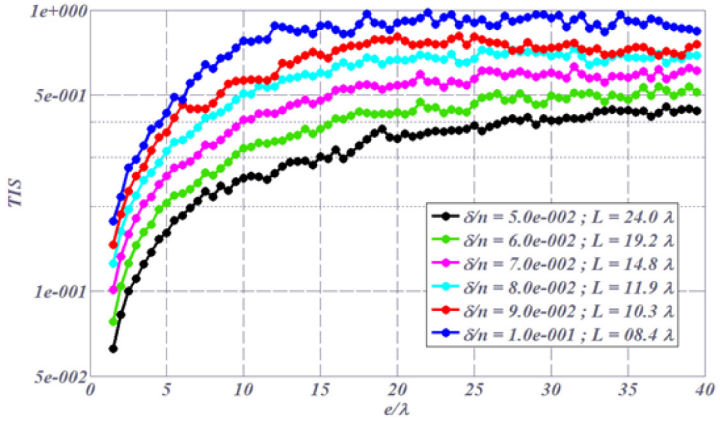

Fig. 3. Mean value of the Total Integrated Scattering in the reflected half-space calculated over 10 realizations and plotted vs the bulk thickness for each index dispersion / mean free path.

Then in our investigation the scattering angle runs from 18° to 50°, so that the specular region (θ *=15°)* is avoided. Notice that the angular resolution largely resolves the speckle,

#228254 - $15.00 USD Received 12 Dec 2014; revised 27 Feb 2015; accepted 4 Mar 2015; published 23 Mar 2015

whose characteristic size calculated as the width at mid-height of the intensity pattern autocorrelation is 2.9° for every couple $\left(\frac{\delta_n}{|\overline{n}|}, d\right)$.

The noticeable speckle size results from the 100λ illumination spot size, a value that was minimized to avoid prohibitive time calculation. As a consequence, the angular investigation range is limited to less than 5 speckle areas for the bulk analysis. For this reason we will not use speckle histograms, contrary to what was done for the surface study [11]. Moreover, previous studies [11, 26] have shown that the knowledge of polarimetric behavior of the scattered field within less than 5 speckles areas is enough to allow to identify the asymptotic behavior of the multiscale degree of polarization MDOP and more precisely to identify the corresponding macroscopic degree of polarization. At last, for all the bulks considered in this paper, 2 speckles areas correspond to an angular aperture greater than 5°, which is enough to quantify the depolarization issues which could occur for imaging applications.

Notice also that invariance of the bulks in one direction is a severe assumption. Hence in this paper's configuration, no cross-polarization is predicted in the plane of incidence, while it should appear for 3D bulks as soon as the perturbative regime is left. However, the Method of Moments gives the rigorous solution of a 1-D wave scattering problem, with all multiple interactions accurately taken into account, which is the point here. In other words, although enpolarization effects cannot be predicted [13–15] under this assumption, great accuracy can be reached for spatial depolarization [11].

Dispersion of the polarization states

Now we use numerical calculation to analyze the polarization states emitted from the bulks. Notations are the following:

$$\begin{aligned} A_S &= \sqrt{I_S}\, e^{j\delta_S} \\ A_P &= \sqrt{I_P}\, e^{j\delta_P} \\ \delta &= \delta_P - \delta_S \end{aligned} \tag{22}$$

with I_S and I_P the polarized speckle patterns and δ the polarimetric phase difference. We also use the amplitude or polarization ratio $\beta = \sqrt{I_P/I_S} = |A_P/A_S|$. These 2 polarization parameters δ and β will allow us to plot the polarization states on the Poincaré sphere.

To discriminate the bulks, two parameters are taken into account, which are the relative index inhomogeneity $\delta_n/|\overline{n}|$ and the thickness of the disturbed bulk. Both parameters were studied independently. On the other hand, the two correlation lengths are taken to be $L_x = L_z =$ 100nm. The thickness varies in the range [1.5λ; 40λ] with a 0.5λ step, while 6 heterogeneities are considered within the interval [0.05; 0.1]. Moreover for each sample, 10 realizations are performed.

As a starting point, the angular variation of the polarization ratio β and the polarimetric phase δ of the resulting fields are plotted Fig. 4 to 7 for 4 representative configurations involving 2 thicknesses (d = 5λ and d = 40λ) and 2 relative inhomogeneities (0.05 and 0.1). Figure 4 and 6 involve 0.05 heterogeneity, while Fig. 6 and 7 are for a 10% heterogeneity. We observe that the root mean square of the polarization ratio increases with thickness, with an average around unity. The same result is obtained for the phase term with an average around zero.

Moreover the phase root mean square clearly increases with the inhomogeneity. With a 5λ thickness, a 10% heterogeneity is required to make the phase uniformly distributed within [0; 2π]; on the other hand, at higher thicknesses, lower heterogeneities allow to approach a uniform phase distribution. Therefore the random nature of the scattered field depends both

#228254 - $15.00 USD Received 12 Dec 2014; revised 27 Feb 2015; accepted 4 Mar 2015; published 23 Mar 2015

on the heterogeneity and the thickness, which is a key difference with the surface scattering process [11].

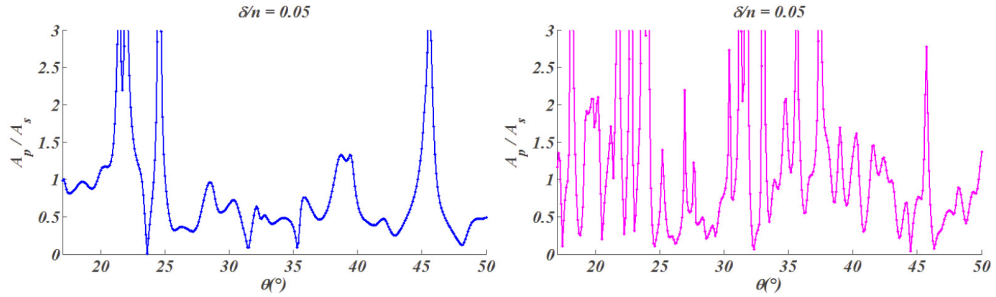

Fig. 4. Polarization ratio for $\delta_n / n = 5.10^{-2}$ and $d = 5\lambda$ (left) and $d = 40\lambda$ (right).

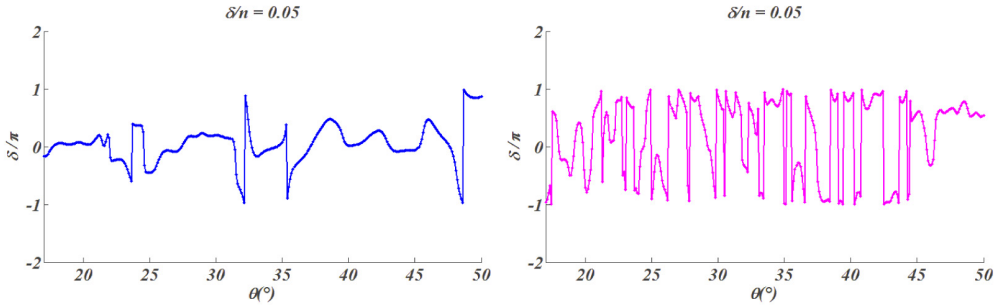

Fig. 5. **:**Polarimetric phase for $\delta_n / n = 5.10^{-2}$ and $d = 5\,\lambda$ (left) and $d = 40\,\lambda$ (right).

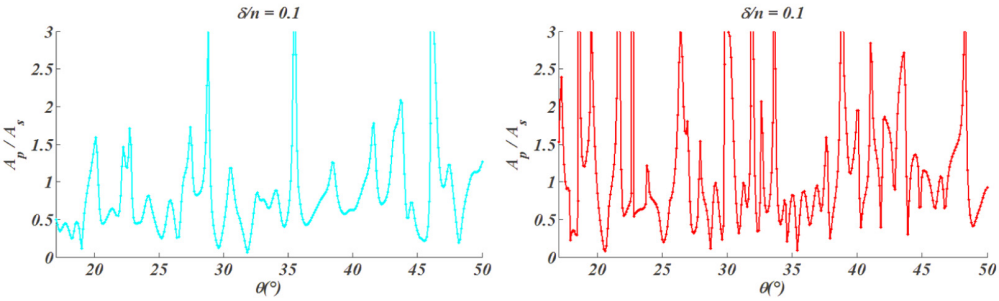

Fig. 6. Polarization ratio for $\delta_n / n = 10^{-1}$ and $d = 5\,\lambda$ (left) and $d = 40\,\lambda$ (right).

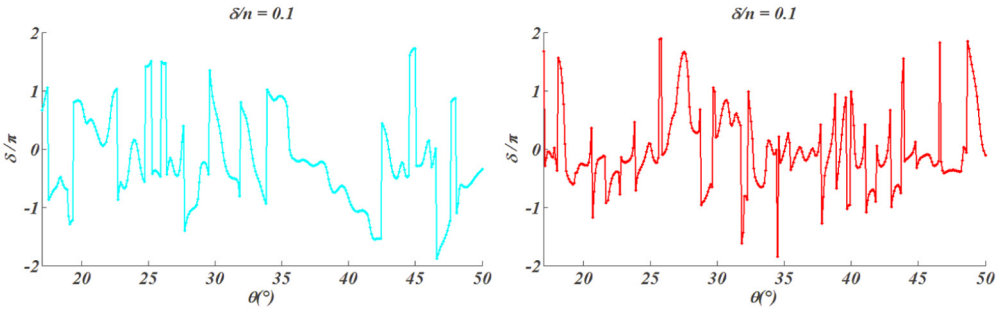

Fig. 7. Polarimetric phase for $\delta_n / n = 10^{-1}$ and $d = 5\,\lambda$ (left) and $d = 40\,\lambda$ (right).

#228254 - $15.00 USD Received 12 Dec 2014; revised 27 Feb 2015; accepted 4 Mar 2015; published 23 Mar 2015

In accordance with the results of Figs. 4-7, the polarization states are plotted on the Poincaré sphere in Figs8-9. Notice at this step that the local (temporal) dop is unity at each point, so that all data points lie at the surface of the sphere. The data cloud on the sphere is directly connected with the sample microstructure and its thickness. Here the angular range includes 3 speckle areas resolved with 100 data points. In Fig. 8 we observe that the dispersion of the states increases with the heterogeneity. Then Fig. 9 shows that dispersion also increases with the thickness.

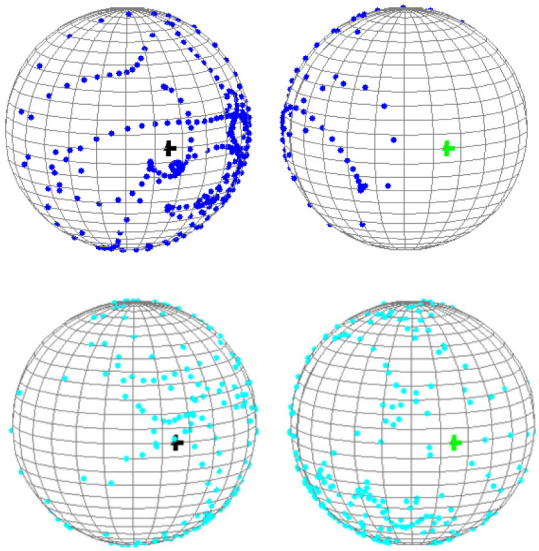

Fig. 8. Dispersion of the polarization states taken by the scattered field on an angular aperture covering 10 speckle areas $d = 5\ \lambda$ *and* $\delta_n / n = 5.10^{-2}$ (top spheres) and 10^{-1} (bottom spheres). Black & green crosses are respectively for L + 45° and L-45° polarization states.

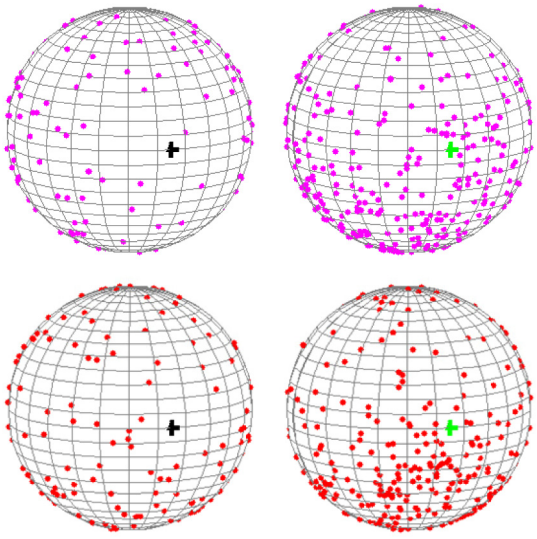

Fig. 9. Dispersion of the polarization states taken by the scattered field on an angular aperture covering 10 speckle areas $d = 40\lambda$ *and* $\delta_n / n = 5.10^{-3}$ (top) and 10^{-1} (bottom). Black & green crosses are respectively for L + 45° an L-45° polarization states.

#228254 - $15.00 USD Received 12 Dec 2014; revised 27 Feb 2015; accepted 4 Mar 2015; published 23 Mar 2015

Spatial depolarization from the bulks

Figures 8 and 9 have revealed the dispersion of the polarization states of the scattered field in less than 3 speckle areas. However these figures do not visualize the path taken by the polarization state when the scattering angle varies continuously. For that reason a complementary view is given in Fig. 10 and shows the continuous variation of the polarization state (Media 1).

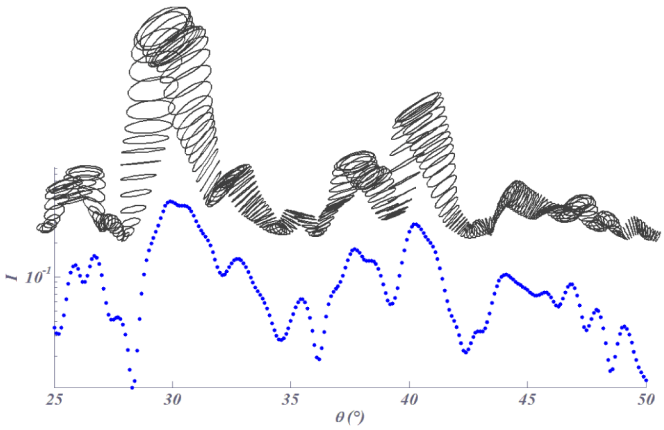

Fig. 10. Continuous variation of the polarization state versus the scattering angle (δ_n / n =5.10^{-2} and $d = 25\lambda$). (Media 1).

Now from Fig. 11 one can expect polarization to fail when several speckle areas are integrated within the receiver aperture $\Delta\Omega$, as predicted in section 2. To quantify such effect we calculated the multi-scale polarization degree $MDOP(\Delta\Omega)$. This function is plotted Fig. 10 for two extreme thicknesses and heterogeneities. In this figure 120 data points (scattering angles) are used; since the speckle area is 29 data points (2.9°), the 120 data points explore 4 speckle areas. The first MDOP value calculated for $\Delta\Omega = 0$ is always unity since no spatial integration has occurred, so that the spatial MDOP equals the temporal dop. Then at higher apertures the dop decreases due to the polarization dispersion. At a given heterogeneity (0.05), the effect is more pronounced at high thickness. However when the heterogeneity increases, the effect of thickness vanishes.

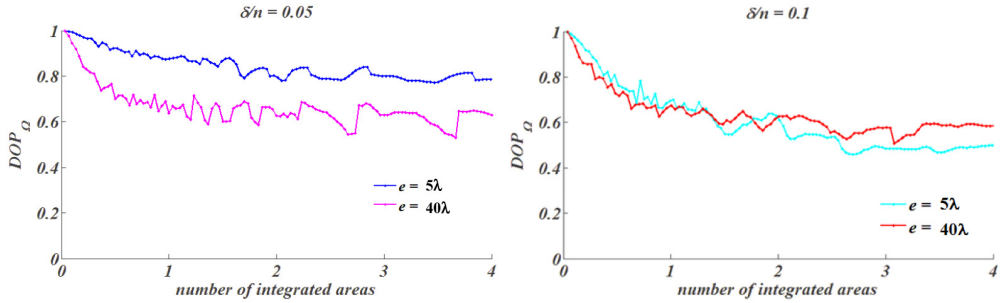

Fig. 11. $MDOP(\Delta\Omega)$ for δ_n / n = 5. 10^{-2} (left) and 10^{-2}(right) for thickness $d = 5\lambda$ and 40λ.

Parametric study

Until now only 2 heterogeneities (0.05 and 0.1) were involved in the polarization analysis from the bulks. To complete the numerical study we studied in this section the variation of

#228254 - $15.00 USD Received 12 Dec 2014; revised 27 Feb 2015; accepted 4 Mar 2015; published 23 Mar 2015

normalized root mean squares (polarization ratio, phase) versus the heterogeneity and thickness. Such quantity is calculated for all parameters are follows:

$$\frac{\sigma_X}{\langle X\rangle}=\frac{1}{\langle X\rangle}\sqrt{\frac{1}{N}\sum_{k=\&}^{N}\left(X-\langle X\rangle\right)^2}\qquad with\ \ X=\beta,\delta \tag{23}$$

Results are given in Figs. 10-13 for the polarization ratio, the polarimetric phase and the degree of polarization. As expected, the β normalized rms increases with thickness, roughly between 0.5 and 2. Concerning the phase, which is distributed between [-π,π] with an average around 0, it varies from 0.2 to 0.5.

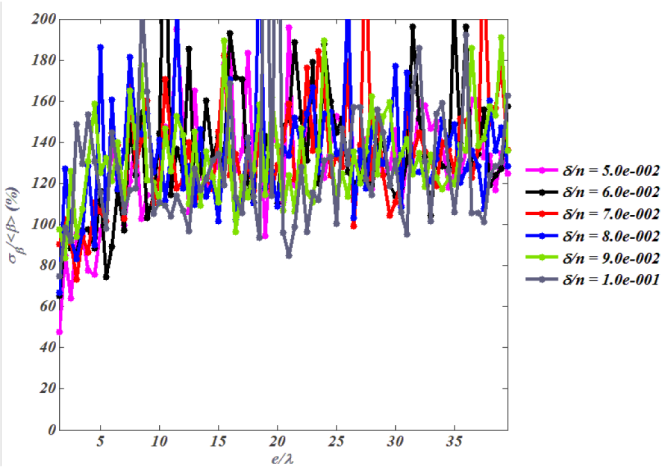

Fig. 12. Normalized Standard deviation of the polarization ratio β versus the relative index inhomogeneity δ_n / n and the thickness *d*.

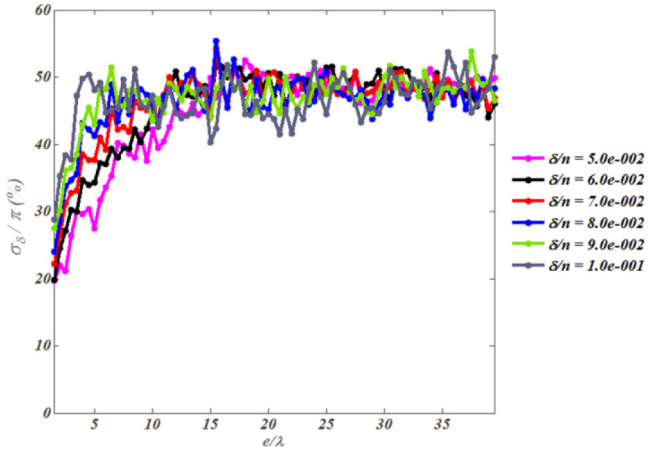

Fig. 13. Standard deviation of the polarimetric phase difference δ normalized by π and expressed versus the relative index inhomogeneity δ_n / n and the thickness *d*.

Such root-mean-squares are responsible for polarization reduction due to the spatial average. In Fig. 14 below we have considered the macroscopic dop, that is, the lower MDOP value obtained for the maximum integration (4 speckle areas). As a first result, one can see

#228254 - $15.00 USD Received 12 Dec 2014; revised 27 Feb 2015; accepted 4 Mar 2015; published 23 Mar 2015

that this asymptotic value decreases with thickness. Furthermore, the slope of the curve around the origins increases with the heterogeneity.

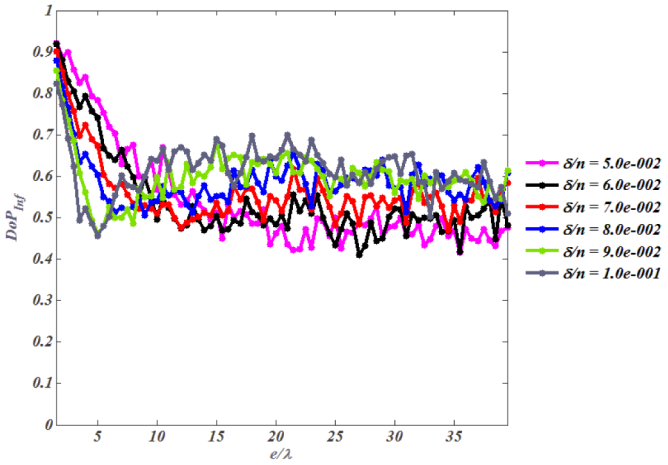

Fig. 14. Macroscopic degree of polarization after integration of 4 speckle areas versus the relative index inhomogeneity δ_n / n and the thickness d.

At last, a linear approximation is proposed Eq. (24) to fit the evolution of the macroscopic degree of polarization as a function of the thickness for each index dispersion $\delta_n / |\overline{n}|$. The linear fits are plotted Fig. 15.

$$DOP_{\inf} \approx 1 - \left| 2 - 100 . \frac{\delta_n}{|\overline{n}|} \right| \overline{n} \frac{e}{50} \tag{24}$$

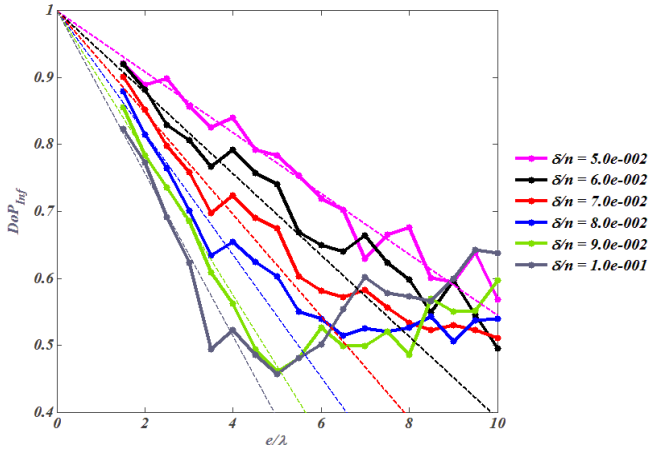

Fig. 15. Zoom- macroscopic degree of polarization and linear approximation after integration of 4 speckle areas versus the relative index inhomogeneity δ_n / n and the thickness d.

Conclusion

The spatial depolarization of light emitted from inhomogeneous bulks was predicted via exact electromagnetic theories. It was shown how full polarization is progressively lost when the heterogeneity increases, and the transition was predicted with an exact electromagnetic theory taking into account the role of the bulk structural parameters.. In a more general way, the

#228254 - $15.00 USD Received 12 Dec 2014; revised 27 Feb 2015; accepted 4 Mar 2015; published 23 Mar 2015

partial degree of polarization was connected to the sample microstructure and geometry. Hence these results devoted to bulk processes can be seen as the continuation of previous results given for surface scattering [11]. We expect the conclusions will be useful in the fields of imaging in complex media, biomedical optics and biophotonics, earth observatory). Moreover, the present work deals with 2D bulks, so that a next step will be to address the 3D geometry which is known to reveal additional phenomena such as temporal repolarization of light [14], a phenomenon which takes its origins in cross-scattering coefficients [15]. The exact calculation of these 3D effects is still in progress but requires huge computational facilities and much more calculation time.

Acknowledgments

This work was performed in the project TraMEL thanks to the financial support of the French National Research Agency. (project # TRAMEL-10-BLAN-0315)

#228254 - $15.00 USD Received 12 Dec 2014; revised 27 Feb 2015; accepted 4 Mar 2015; published 23 Mar 2015